Supplement of Atmos. Meas. Tech., 17, 2917–2936, 2024
https://doi.org/10.5194/amt-17-2917-2024-supplement

Atmospheric Measurement Techniques
Open Access
EGU

Supplement of

Field comparison of dual- and single-spot Aethalometers: equivalent black carbon, light absorption, Ångström exponent and secondary brown carbon estimations

Liangbin Wu et al.

Correspondence to: Cheng Wu (wucheng.vip@foxmail.com)

Test S1 AAE calculation examples

Following are the data points used as an example.

babs370	babs470	babs520	babs590	babs660	babs880	babs950
41.98	32.19	27.40	24.04	20.45	14.27	13.52
ln(babs370)	ln(babs 470)	ln(babs520)	ln(babs590)	ln(babs660)	ln(babs880)	ln(babs950)
3.74	3.47	3.31	3.18	3.02	2.66	2.60
λ1	λ2	λ3	λ4	λ5	λ6	λ7
370	470	520	590	660	880	950
ln370	ln470	ln520	ln590	ln660	ln880	ln950
5.91	6.15	6.25	6.38	6.49	6.78	6.86

Example of approach 1:

$$AAE_{370/950} = \frac{\ln\left(b_{abs950}/b_{abs370}\right)}{\ln\left(370/950\right)}$$

$AAE_{370/950}$=ln(13.52/41.98)/ln(370/950)=1.20

Example of approach 2:

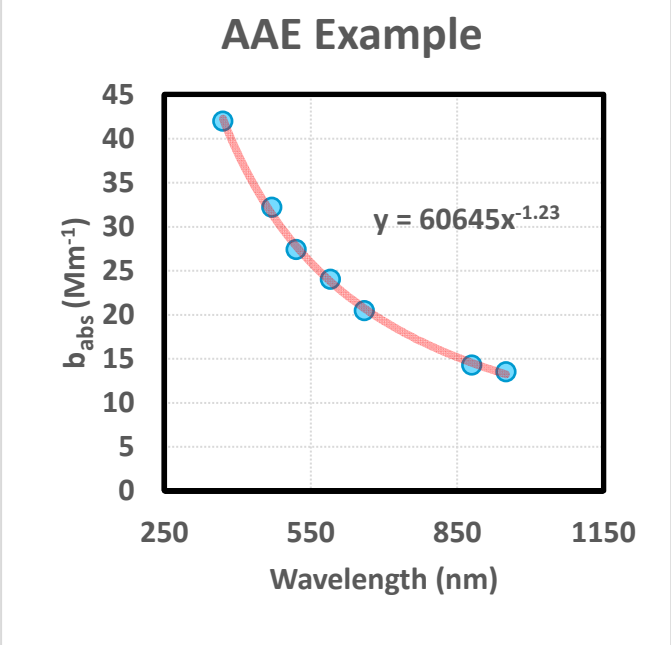

AAE wave obtained from the curve fitting of the power function. In this case, $AAE_{370-950} = 1.23$

Table S1. The σ_{air} of AE33 Aethalometer and σ_{ATN} of AE31 Aethalometer. The relationship between σ_{air} and σ_{ATN} can be written as $\sigma_{ATN} = C_0 \cdot \sigma_{air}$. The σ_{air} was derived from the historical σ_{ATN} using $C_0 = 2.14$ (Drinovec et al., 2015).

Wavelength	**AE33_σ_{air} (m^2g^{-1})**	**AE31_σ_{ATN} (m^2g^{-1})**
370 nm	18.47	39.5
470 nm	14.54	31.1
520 nm	13.14	28.1
590 nm	11.58	24.8
660 nm	10.35	22.2
880 nm	7.77	16.6
950 nm	7.19	15.4

Table S2. Summary of the multiple scattering parameter (C_{ref}) values for Aethamometers reported in the literature.

Reference	Site	Site type	Aethalometer (Filter type)	Reference instrument	Wavelength (nm)						
					370	470	520	590	660	880	950
(Bernardoni et al., 2021)	Milan (Italy)	Urban background station	AE33 (TFE-coated glass fibre tape T60A20)	PP_UniMI		2.91	2.93		2.78	2.78	
			AE31 (Pall Q250 quartz)			3.58	3.54		3.56	3.47	
(Valentini et al., 2020)	Rome (Italy)	Urban background station	AE33	MAAP					2.66		
(Zhao et al., 2020)	Beijing (China)	Urban	AE33 (Tape 8060)	PASS-3				2.9 ± 0.4			
(Backman et al., 2017)	Arctic	Clean environment	AE31 (Pallflex Q250F)	PSAP/MAAP				3.45			
(Di Biagio et al., 2017)	Laboratory	Mineral dust aerosols	AE31	Extinction minus scattering					1.92		
(Segura et al., 2014)	Granada (Spain)	Urban	AE31	MAAP	3.42	3.87	3.90	3.98	4.19	4.35	4.59
(Arnott et al., 2005)	Las Vegas (USA)	Urban	AE31	PAS			3.69				
(Collaud Coen et al., 2010)	Cabauw, (Netherlands)	Urban	AE31 (Pallflex Q250F)	MAAP					4.26		
(Zhang et al., 2021)	Beijing (China)	Urban	AE31	PAS	5.61	4.98	4.73	4.92	5.19	5.30	5.24
(Weingartner et al., 2003)	Laboratory	Diesel soot with organic coating	AE30 (Pallflex Q250F)	Extinction minus scattering					3.60		
(Schmid et al., 2006)	Amazon (Brazil)	Biomass aerosol	AE30	PAS			5.23				
(Saturno et al., 2017)	Amazon (Brazil)	Urban	AE31	MAPP					4.90		
(Lim et al., 2018)	East Asia	Urban	AE31	PASS-3	3.37	3.80	3.99	4.25	4.49	5.18	5.39
(Ajtai et al., 2019)	Budapest (Hungary)	Urban	AE42 (Quartz)	PAS	2.15	3.52	4.78	4.86	5.21	5.11	5.16
(Laing et al., 2020)	Oregon (USA)	Rural	AE33 (TFE-coated glass filter)	TAP		4.35	4.45		4.24		
(Qin et al., 2018)	Guangzhou (China)	Suburban	AE33 (TFE-coated glass filter)	Extinction minus scattering	$C_{AE33} = C_0 \cdot H$ = 1.57·2.1 = 3.297						
(Wu et al., 2013)	Guangzhou (China)	Suburban	AE16	PAS				3.48			

Table S3. The monthly eBC mass concentrations (μg m^{-3}) of AE31 and AE33 Aethalometers at 5 min and 1 hr time bases. AE31_V and AE31_W are AE31 data corrected by algorithms of Virkkula and Weingartner, respectively. $AE33_{2nd\_Cor}$ refers to eBC of AE33 with the second correction.

Time base	Instrument/ Algorithm	Annual	Apr-2021	May-2021	Jun-2021	Jul-2021	Aug-2021	Sep-2021	Oct-2021	Nov-2021	Dec-2021	Jan-2022	Feb-2022	Mar-2022
1 hr	AE31_V	1.95±1.12	2.44±1.14	1.75±0.91	1.89±0.86	1.66±0.80	1.98±0.90	2.26±1.06	1.39±0.83	1.71±0.92	2.05±1.16	2.63±1.53	1.18±0.90	2.38±1.24
	AE31_W	1.95±1.12	2.44±1.15	1.75±0.91	1.89±0.86	1.66±0.81	1.98±0.90	2.26±1.07	1.38±0.84	1.70±0.92	2.04±1.16	2.62±1.50	1.17±0.90	2.38±1.24
	AE33	2.35±1.37	2.76±1.29	2.06±1.05	2.22±1.05	1.91±0.85	2.36±1.10	2.65±1.24	1.81±1.16	2.21±1.26	2.51±1.39	3.25±1.86	1.46±1.16	2.91±1.65
	$AE33_{2nd\_Cor}$	1.96±1.14	2.30±1.08	1.71±0.87	1.85±0.87	1.59±0.71	1.97±0.92	2.21±1.04	1.51±0.97	1.84±1.05	2.09±1.16	2.71±1.55	1.22±0.97	2.43±1.38
5 min	AE31_V	1.96±1.18	2.45±1.21	1.75±0.95	1.89±0.93	1.66±0.85	1.97±0.95	2.25±1.10	1.39±0.84	1.71±0.93	2.05±1.23	2.63±1.62	1.18±0.95	2.42±1.31
	AE31_W	1.96±1.18	2.46±1.22	1.75±0.96	1.89±0.94	1.66±0.85	1.98±0.95	2.25±1.12	1.39±0.85	1.71±0.94	2.05±1.23	2.62±1.62	1.17±0.96	2.41±1.31
	AE33	2.35±1.39	2.78±1.37	2.05±1.07	2.22±1.09	1.91±0.89	2.36±1.13	2.64±1.27	1.79±1.14	2.18±1.19	2.52±1.43	3.25±1.87	1.46±1.16	2.91±1.66
	$AE33_{2nd\_Cor}$	2.02±1.20	2.36±1.16	1.74±0.90	1.88±0.92	1.61±0.75	2.00±0.96	2.24±1.08	1.52±0.97	1.85±1.00	2.13±1.21	2.80±1.61	1.26±1.00	2.51±1.43

Table S4. Annual mean b_{abs} (±1 S.D.)by AE31_V, AE31_W and AE33 at 7 wavelengths.

Model	Time base	Annual mean b_{abs} with ±1 S.D. (Mm^{-1})						
		370 nm	470 nm	520 nm	590 nm	660 nm	880 nm	950 nm
AE31_V	1 hr	22.10±12.78	16.94±9.84	14.72±8.58	13.12±7.70	11.75±6.94	8.69±5.20	7.69±4.63
	5 min	22.16±13.03	16.98±10.55	14.76±8.78	13.15±7.90	11.78±7.15	7.81±5.42	7.71±4.86
AE31_W	1 hr	20.62±11.97	16.36±9.51	14.47±8.44	12.97±7.63	11.49±6.80	8.62±5.19	7.51±4.55
	5 min	20.70±12.22	16.42±9.73	14.52±8.65	13.02±7.84	11.53±7.01	8.65±5.41	7.54±4.79
AE33	1 hr	21.05±12.48	16.33±9.59	14.05±7.90	12.21±7.19	10.42±6.15	7.51±4.48	7.14±4.27
	5 min	21.04±12.64	16.32±9.70	14.02±8.10	12.20±7.27	10.41±6.23	7.50±4.54	7.14±4.32

Table S5. Monthly b_{abs} comparisons (370 nm) among AE33_b_{abs}, AE31_V_b_{abs}, and AE31_W_b_{abs} at 5 min and 1 hr time bases. Where the AE31_V_b_{abs} and AE31_W_b_{abs} are the light absorption coefficients of AE31 corrected by the procedures of Virkkula and Weingartner, respectively. And the AE33_b_{abs} is the light absorption coefficient of the AE33 aethalometer.

370 nm	Time base		Annual	Apr-2021	May-2021	Jun-2021	Jul-2021	Aug-2021	Sep-2021	Oct-2021	Nov-2021	Dec-2021	Jan-2022	Feb-2022	Mar-2022
AE33_b_{abs} vs AE31_V_b_{abs}	5 min	R^2	0.95	0.96	0.97	0.95	0.93	0.95	0.94	0.93	0.93	0.97	0.93	0.94	0.91
		Slope	0.96	0.89	0.91	0.92	0.85	0.95	0.97	0.98	1.03	0.98	0.97	0.98	1.00
	1 hr	R^2	0.96	0.96	0.98	0.98	0.97	0.96	0.96	0.97	0.96	0.98	0.97	0.97	0.96
		Slope	0.97	0.89	0.93	0.93	0.89	0.96	0.99	1.06	1.09	0.99	0.98	0.97	1.08
AE33_b_{abs} vs AE31_W_b_{abs}	5 min	R^2	0.94	0.95	0.96	0.94	0.93	0.94	0.93	0.93	0.91	0.96	0.91	0.94	0.89
		Slope	1.03	0.95	0.97	1.00	0.90	1.02	1.04	1.05	1.10	1.05	1.04	1.04	1.07
	1 hr	R^2	0.95	0.95	0.97	0.97	0.96	0.95	0.95	0.96	0.95	0.97	0.96	0.96	0.95
		Slope	1.04	0.96	0.99	1.01	0.95	1.03	1.05	1.14	1.16	1.05	1.06	1.04	1.15
AE31_W_b_{abs} vs AE31_V_b_{abs}	5 min	R^2	0.99	0.99	0.99	0.99	0.99	0.99	0.99	0.99	0.99	0.99	0.99	0.99	0.99
		Slope	0.93	0.94	0.94	0.92	0.94	0.93	0.94	0.93	0.94	0.94	0.93	0.94	0.94
	1 hr	R^2	0.99	0.99	0.99	0.99	0.99	0.99	0.99	0.99	0.99	0.99	0.99	0.99	0.99
		Slope	0.93	0.93	0.94	0.92	0.94	0.93	0.94	0.93	0.94	0.94	0.93	0.93	0.94

Table S6. Monthly b_{abs} comparisons (880 nm) among AE33_b_{abs}, AE31_V_b_{abs}, and AE31_W_b_{abs} at 5 min and 1 hr time bases. Where the AE31_V_b_{abs} and AE31_W_b_{abs} are the light absorption coefficients of AE31 corrected by the procedures of Virkkula and Weingartner, respectively. And the AE33_b_{abs} is the light absorption coefficient of the AE33 aethalometer.

880 nm	Time base		Annual	Apr-2021	May-2021	Jun-2021	Jul-2021	Aug-2021	Sep-2021	Oct-2021	Nov-2021	Dec-2021	Jan-2022	Feb-2022	Mar-2022
AE33_b_{abs}	5 min	R^2	0.91	0.94	0.90	0.88	0.89	0.91	0.92	0.93	0.86	0.92	0.84	0.87	0.84
vs		Slope	0.85	0.77	0.72	0.74	0.74	0.80	0.80	0.88	0.91	0.83	0.84	0.86	0.86
AE31_V_b_{abs}	1 hr	R^2	0.97	0.97	0.97	0.97	0.96	0.97	0.96	0.97	0.96	0.98	0.98	0.98	0.97
		Slope	0.87	0.81	0.85	0.86	0.79	0.88	0.85	0.95	0.96	0.87	0.89	0.87	0.99
AE33_b_{abs}	5 min	R^2	0.91	0.93	0.89	0.86	0.88	0.90	0.90	0.92	0.86	0.92	0.84	0.87	0.84
vs		Slope	0.86	0.77	0.72	0.75	0.75	0.80	0.80	0.89	0.92	0.83	0.85	0.87	0.87
AE31_W_b_{abs}	1 hr	R^2	0.96	0.96	0.96	0.96	0.94	0.96	0.95	0.96	0.95	0.98	0.98	0.97	0.97
		Slope	0.95	0.81	0.85	0.86	0.80	0.88	0.85	0.96	0.97	0.88	0.91	0.88	1.01
AE31_W_b_{abs}	5 min	R^2	0.99	0.99	0.99	0.99	0.99	0.99	0.99	0.99	0.99	0.99	0.99	1.00	0.99
vs		Slope	0.99	1.00	0.99	0.99	0.99	1.00	1.00	0.99	0.99	0.99	0.99	0.98	0.99
AE31_V_b_{abs}	1 hr	R^2	1.00	0.99	0.99	0.99	0.99	0.99	0.99	0.99	0.99	0.99	0.99	1.00	0.99
		Slope	0.98	1.00	1.00	1.00	0.99	1.00	1.00	0.98	0.99	0.99	0.99	1.00	0.99

Table S7. The relative deviation of slope between monthly and annual data among AE33_b_{abs}, AE31_V_b_{abs}, and AE31_W_b_{abs} at 5 min and 1 hr time bases. The month with the maximum deviation was shown in bold. Where the AE31_V_b_{abs} and AE31_W_b_{abs} are the light absorption coefficients of AE31 corrected by the procedures of Virkkula and Weingartner, respectively. And the AE33_b_{abs} is the light absorption coefficient of the AE33 aethalometer.

Relative deviation of slope	Instrument/ Algorithm	Time base	Apr-2021	May-2021	Jun-2021	Jul-2021	Aug-2021	Sep-2021	Oct-2021	Nov-2021	Dec-2021	Jan-2022	Feb-2022	Mar-2022
370 nm	**AE33_b_{abs} vs AE31_V_b_{abs}**	5 min	7.29%	5.21%	4.17%	**11.46%**	1.04%	1.04%	2.08%	7.29%	2.08%	1.04%	2.08%	4.17%
		1 hr	8.25%	4.12%	4.12%	8.25%	1.03%	2.06%	9.28%	**12.37%**	2.06%	1.03%	0.00%	11.34%
	AE33_b_{abs} vs AE31_W_b_{abs}	5 min	7.77%	5.83%	2.91%	**12.62%**	0.97%	0.97%	1.94%	6.80%	1.94%	0.97%	0.97%	3.88%
		1 hr	7.69%	4.81%	2.88%	8.65%	0.96%	0.96%	9.62%	**11.54%**	0.96%	1.92%	0.00%	10.58%
	AE31_W_b_{abs} vs AE31_V_b_{abs}	5 min	1.08%	1.08%	1.08%	1.08%	0.00%	1.08%	0.00%	1.08%	1.08%	0.00%	1.08%	1.08%
		1 hr	0.00%	1.08%	1.08%	1.08%	0.00%	1.08%	0.00%	1.08%	1.08%	0.00%	0.00%	1.08%
880 nm	**AE33_b_{abs} vs AE31_V_b_{abs}**	5 min	9.41%	15.29%	**12.94%**	**12.94%**	5.88%	5.88%	3.53%	7.06%	2.35%	1.18%	1.18%	1.18%
		1 hr	6.90%	2.30%	1.15%	9.20%	1.15%	2.30%	9.20%	10.34%	0.00%	2.30%	0.00%	**13.79%**
	AE33_b_{abs} vs AE31_W_b_{abs}	5 min	10.47%	**16.28%**	12.79%	12.79%	6.98%	6.98%	3.49%	6.98%	3.49%	1.16%	1.16%	1.16%
		1 hr	6.90%	2.30%	1.15%	8.05%	1.15%	2.30%	10.34%	11.49%	1.15%	4.60%	1.15%	**16.09%**
	AE31_W_b_{abs} vs AE31_V_b_{abs}	5 min	1.01%	0.00%	0.00%	0.00%	1.01%	1.01%	0.00%	0.00%	0.00%	0.00%	1.01%	0.00%
		1 hr	1.01%	1.01%	1.01%	0.00%	1.01%	1.01%	1.01%	0.00%	0.00%	0.00%	1.01%	0.00%

Table S8. Sensitivity test of C value on the comparison of AE33 vs. AE31. The value of C_{AE33} was varied from 2.419 to 3.319 with an interval of 0.1 while C_{AE31} was set to a constant (3.48) during the sensitivity test.

	AE33/AE31 slope							
C_{AE33}	370 nm	470 nm	520 nm	590 nm	660 nm	880 nm	950 nm	Average
2.419	1.17	1.17	1.05	1.13	1.08	1.04	1.13	1.11
2.519	1.12	1.13	1.01	1.09	1.03	1.00	1.08	1.07
2.619	1.08	1.08	0.97	1.04	0.99	0.96	1.04	1.02
2.719	1.04	1.04	0.93	1.01	0.96	0.93	1.00	0.99
2.819	1.00	1.01	0.90	0.97	0.92	0.90	0.97	0.95
2.919	0.97	0.97	0.87	0.94	0.89	0.87	0.93	0.92
3.019	0.93	0.94	0.84	0.91	0.86	0.84	0.90	0.89
3.119	0.90	0.91	0.81	0.88	0.84	0.81	0.87	0.86
3.219	0.88	0.88	0.79	0.85	0.81	0.79	0.85	0.84
3.319	0.85	0.85	0.76	0.82	0.78	0.76	0.82	0.81

Table S9. Monthly average (±1 S.D.) of AAE values ($AAE_{470/660}$, $AAE_{370/880}$, $AAE_{880/950}$, $AAE_{370/950}$ and $AAE_{370\text{-}950}$) calculated by 1 hr data.

AAE		Apr-2021	May-2021	Jun-2021	Jul-2021	Aug-2021	Sep-2021	Oct-2021	Nov-2021	Dec-2021	Jan-2022	Feb-2022	Mar-2022	Annual
470/660	AE31_V	1.04±0.09	1.03±0.08	1.04±0.08	1.03±0.08	1.03±0.08	1.01±0.08	1.09±0.14	1.20±0.18	1.22±0.11	1.23±0.09	1.30±0.18	1.17±0.11	1.12±0.15
	AE31_W	1.00±0.13	1.00±0.12	1.00±0.13	1.00±0.13	0.99±0.12	0.98±0.12	1.06±0.17	1.17±0.19	1.18±0.14	1.19±0.12	1.28±0.19	1.13±0.14	1.08±0.17
	AE33	1.28±0.08	1.25±0.05	1.27±0.07	1.28±0.06	1.27±0.06	1.27±0.06	1.33±0.09	1.40±0.12	1.43±0.09	1.45±0.09	1.46±0.14	1.34±0.14	1.33±0.12
370/880	AE31_V	1.04±0.15	1.03±0.26	1.03±0.23	1.03±0.17	1.02±0.20	1.01±0.15	1.09±0.24	1.21±0.29	1.23±0.20	1.25±0.22	1.28±0.27	1.16±0.23	1.11±0.14
	AE31_W	0.97±0.18	0.96±0.28	0.96±0.25	0.96±0.20	0.95±0.22	0.94±0.18	1.02±0.26	1.15±0.31	1.16±0.22	1.18±0.23	1.23±0.28	1.09±0.25	1.05±0.17
	AE33	1.12±0.11	1.11±0.06	1.12±0.08	1.14±0.07	1.12±0.07	1.13±0.07	1.21±0.10	1.27±0.12	1.31±0.09	1.32±0.10	1.30±0.20	1.21±0.15	1.20±0.13
880/950	AE31_V	1.59±0.32	1.72±0.41	1.74±0.39	1.65±0.34	1.69±0.38	1.67±0.38	1.85±0.49	1.74±0.56	1.77±0.38	1.98±0.57	1.82±0.61	1.78±0.57	1.75±0.47
	AE31_W	1.78±0.31	1.91±0.40	1.94±0.38	1.84±0.34	1.89±0.37	1.86±0.37	2.04±0.49	1.92±0.52	1.95±0.38	2.17±0.57	1.99±0.60	1.96±0.57	1.94±0.46
	AE33	0.66±0.06	0.62±0.06	0.62±0.06	0.62±0.06	0.60±0.05	0.62±0.06	0.65±0.09	0.69±0.10	0.72±0.07	0.76±0.11	0.76±0.28	0.67±0.13	0.67±0.12
370/950	AE31_V	1.05±0.07	1.02±0.06	1.03±0.07	1.04±0.06	1.03±0.06	1.03±0.06	1.10±0.09	1.18±0.14	1.22±0.10	1.23±0.09	1.26±0.11	1.14±0.10	1.16±0.14
	AE31_W	1.01±0.11	0.98±0.10	0.99±0.11	1.00±0.11	0.98±0.10	0.98±0.11	1.06±0.13	1.15±0.16	1.18±0.13	1.19±0.11	1.23±0.14	1.09±0.13	1.12±0.17
	AE33	1.12±0.08	1.10±0.05	1.11±0.06	1.12±0.06	1.11±0.05	1.12±0.06	1.20±0.09	1.25±0.10	1.29±0.08	1.32±0.09	1.35±0.14	1.20±0.13	1.15±0.12
370-950	AE31_V	1.06±0.16	1.06±0.29	1.06±0.28	1.05±0.19	1.05±0.23	1.04±0.18	1.12±0.26	1.22±0.31	1.24±0.22	1.28±0.29	1.30±0.26	1.19±0.26	1.11±0.12
	AE31_W	1.02±0.19	1.02±0.31	1.02±0.29	1.01±0.21	1.01±0.25	1.00±0.20	1.08±0.27	1.18±0.32	1.20±0.23	1.24±0.30	1.27±0.27	1.14±0.27	1.07±0.15
	AE33	1.12±0.08	1.10±0.05	1.11±.0.06	1.12±0.06	1.11±0.06	1.12±0.06	1.19±0.10	1.25±0.11	1.29±0.09	1.31±0.10	1.35±0.17	1.20±0.15	1.19±0.12

Table S10. Secondary brown carbon light absorption of AE31 and AE33 aethalometers at hourly time resolution.

b_{abs370_BrCsec} (Mm^{-1})	AE31_V	AE31_W	AE33
Full-year	2.16 ± 2.02	2.61 ± 2.35	1.99 ± 1.97
Dry season	2.68 ± 2.15	2.91 ± 2.54	2.34 ± 2.08
Wet season	1.12 ± 1.15	2.07 ± 1.85	0.99 ± 1.15
Apr-2021	1.85 ± 1.51	2.80 ± 2.42	1.55 ± 1.65
May-2021	0.71 ± 0.62	1.58 ± 1.41	0.43 ± 0.44
Jun-2021	0.96 ± 1.14	1.89 ± 1.72	0.82 ± 1.03
Jul-2021	0.98 ± 1.07	1.87 ± 1.63	0.87 ± 0.91
Aug-2021	0.92 ± 0.87	2.05 ± 1.73	0.86 ± 0.79
Sep-2021	1.08 ± 0.99	2.11 ± 1.71	1.05 ± 1.06
Oct-2021	1.44 ± 1.58	1.94 ± 1.80	1.58 ± 1.82
Nov-2021	3.46 ± 2.39	3.66 ± 2.90	2.95 ± 2.37
Dec-2021	4.22 ± 2.40	4.51 ± 3.06	3.38 ± 2.38
Jan-2022	3.02 ± 1.78	3.08 ± 2.19	2.38 ± 1.77
Feb-2022	1.64 ± 1.28	1.67 ± 1.40	1.45 ± 1.32
Mar-2022	1.92 ± 1.56	2.27 ± 2.01	1.75 ± 1.62

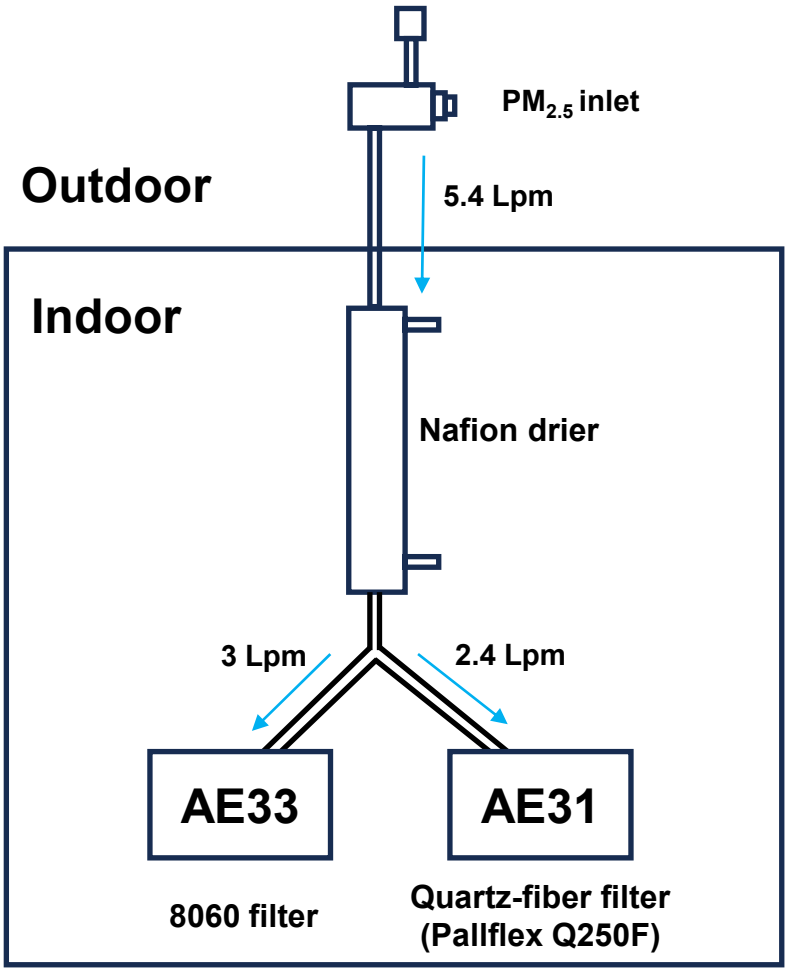

Figure S1. Tubing connection diagram of AE33 and AE31.

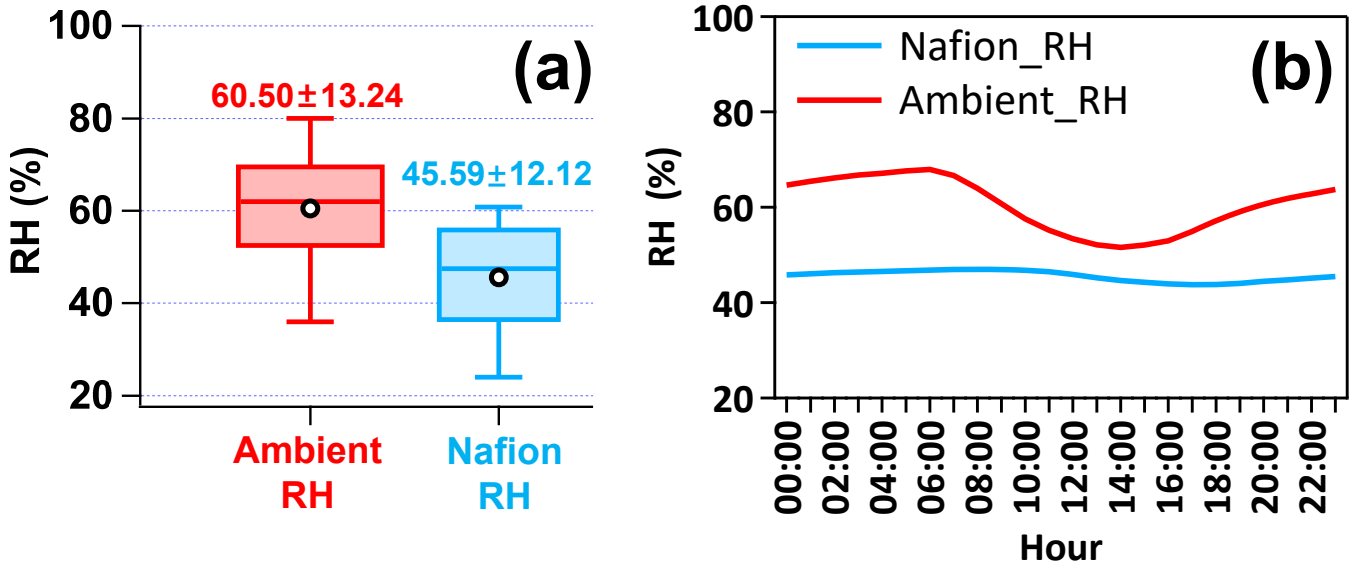

Figure S2. Ambient and dried sample RH (Nafion) characteristics during the one-year campaign. (a) Box plot of annual average RH. Black circles represent annual average concentrations. The line inside the box indicates the annual median concentration. The upper and lower boundaries of the box represent the 75th and the 25th percentile; the whisker above and below each box represents the 95th and 5th percentile. (b) Diurnal variations of ambient and Nafion RH.

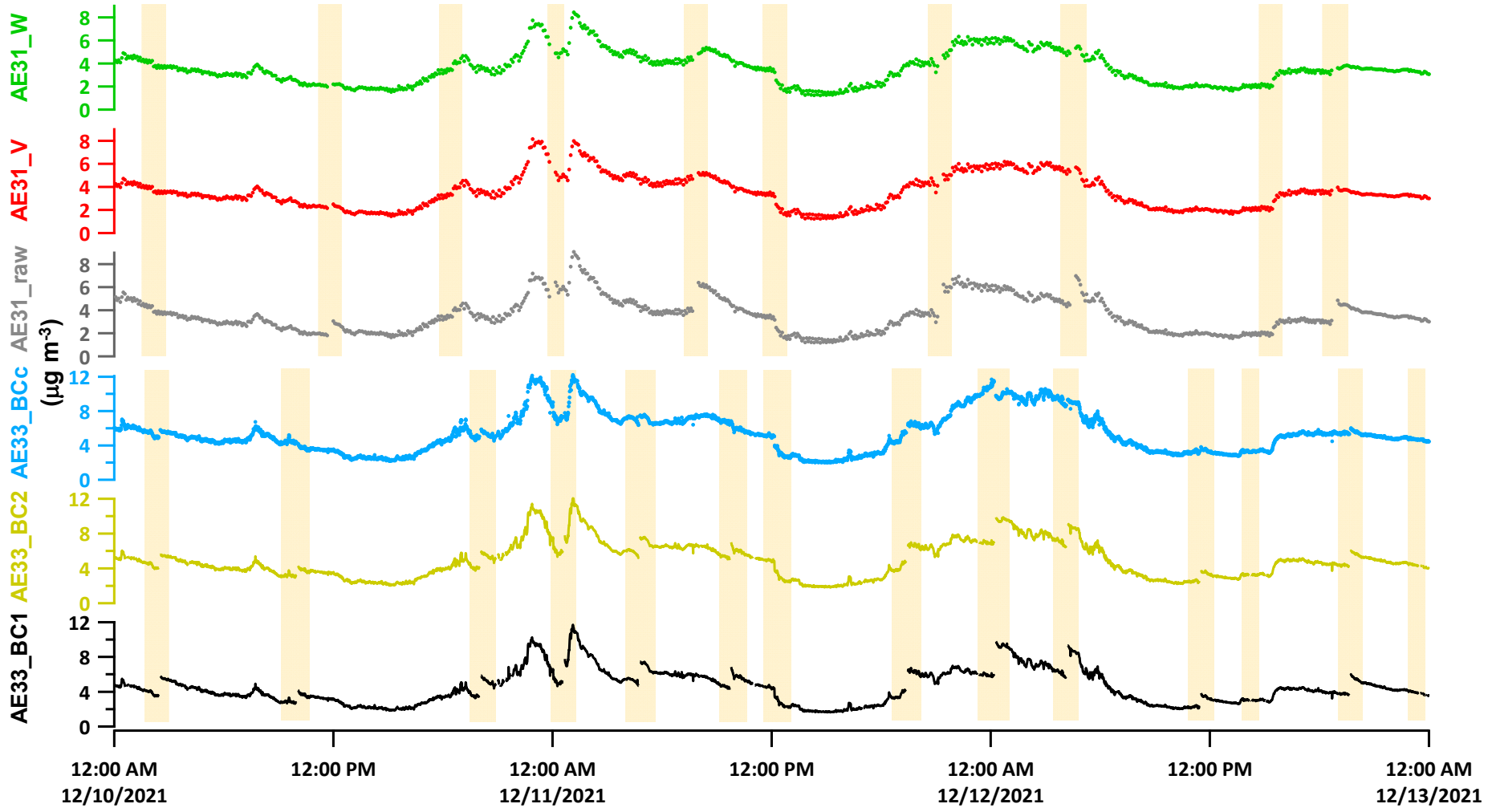

Figure S3. Example of Aethalometer eBC data before and after correction. The shaded areas indicate the change of sampling spot to a new position. AE31_V and AE31_W represent AE31 data corrected by Virkkula and Weingartner algorithms, respectively.

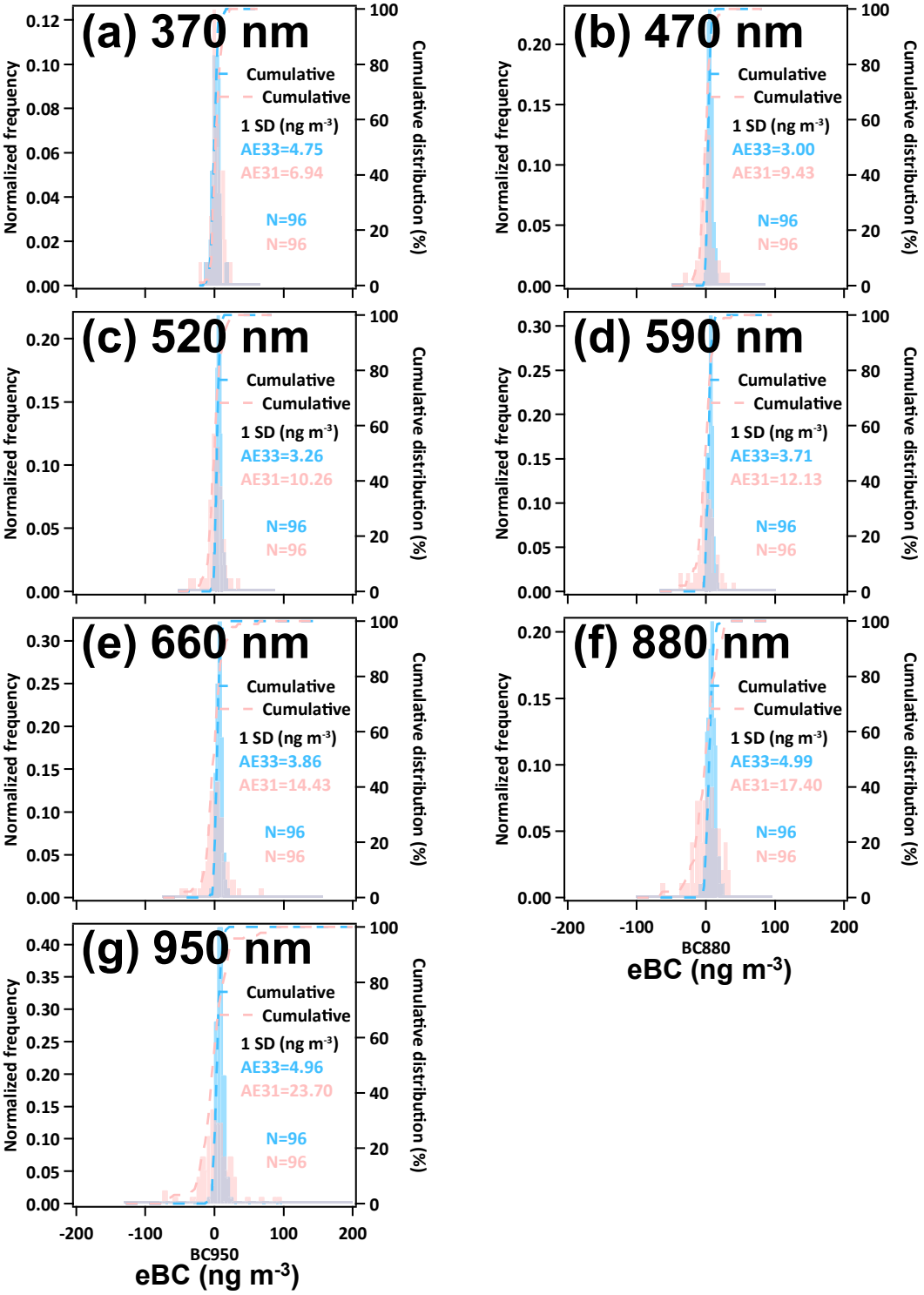

Figure S4. The frequency histograms of the blank measurements of AE31 and AE33 at the time base of 60 min. The red histograms represent AE31 and AE33 results are shown in blue histograms. Figures a-g correspond to 370, 470, 520, 590, 660, 880 and 950 nm, respectively.

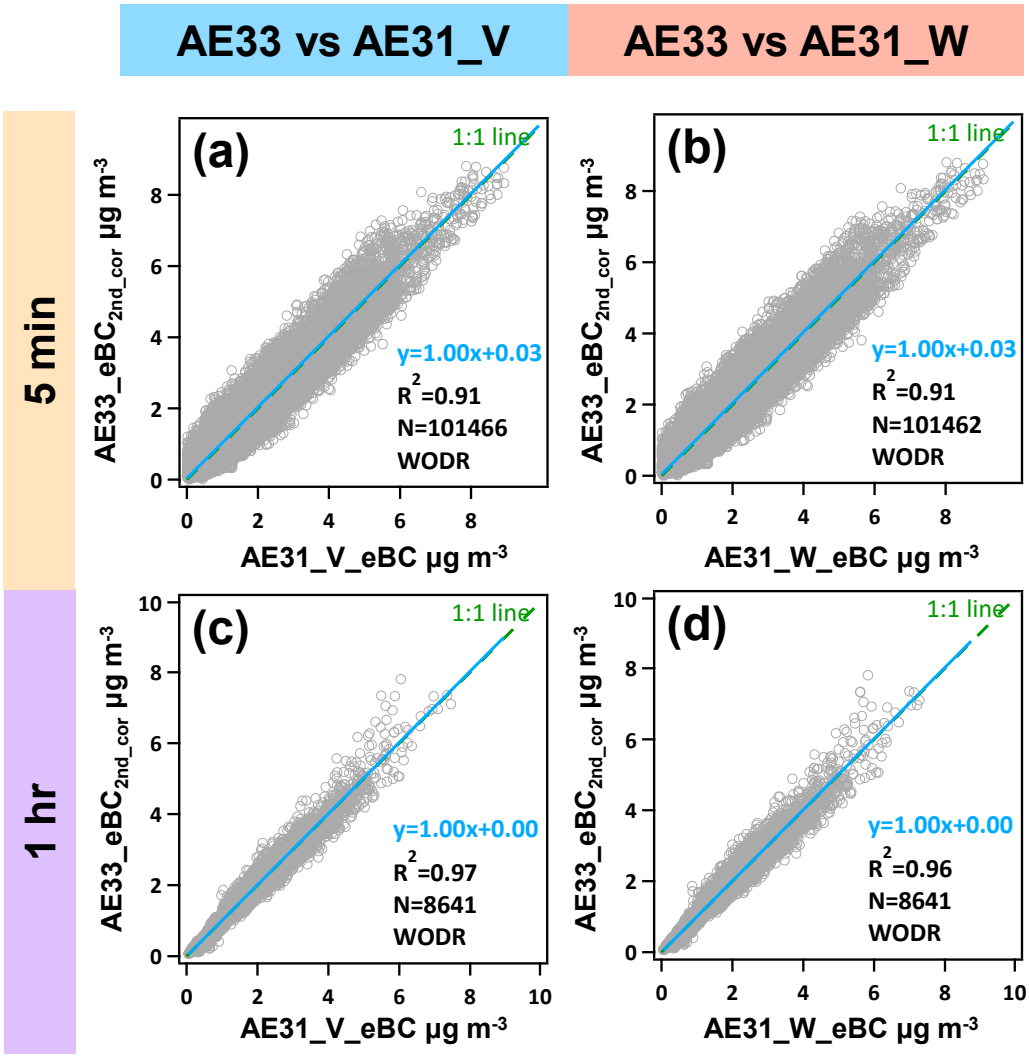

Figure S5. The 2nd-correction eBC mass concentration comparison between AE33 data and AE31 data at 5 min and 1 hr time base.

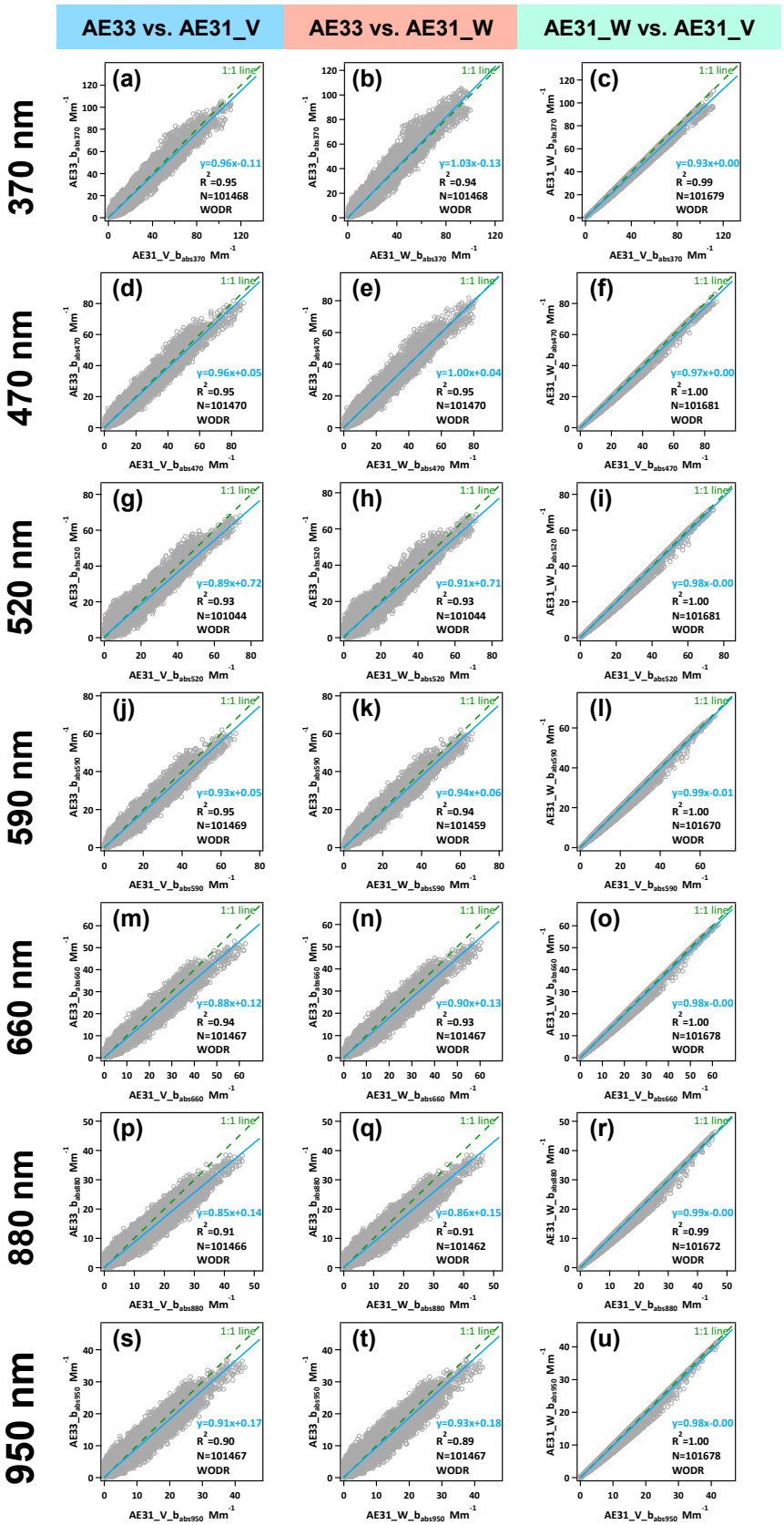

Figure S6. Comparisons of 5 min light absorption coefficient between AE33 and AE31 at 370, 470, 520, 590, 660, 880 and 950 nm. AE31_V_b_{abs} and AE31_W_b_{abs} represent the light absorption coefficients of AE31 corrected by the algorithms of Virkkula and Weingartner, respectively.

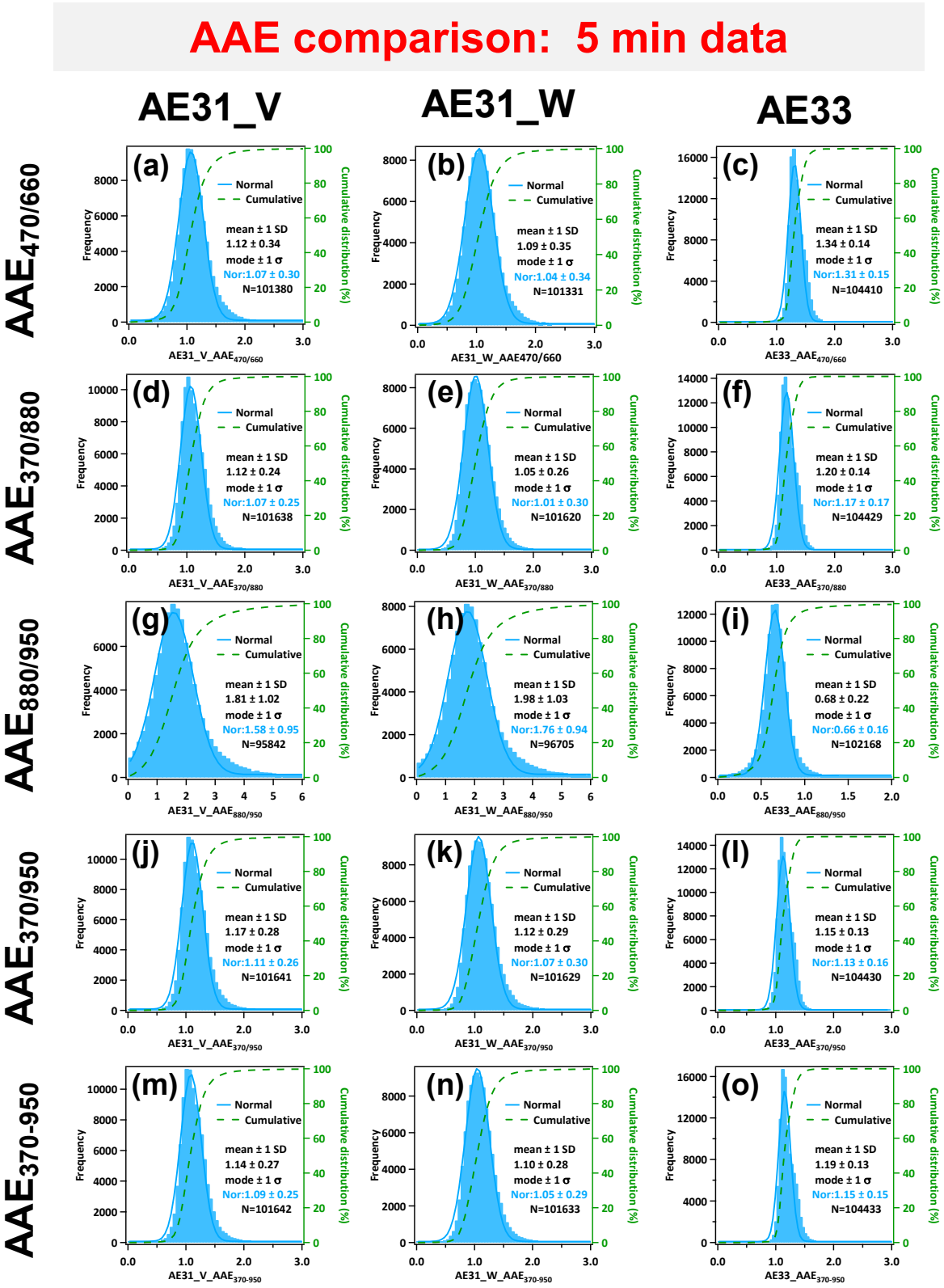

Figure S7. Frequency distributions of AAE values of AE33, AE31_V (AE31 data corrected by Virkkula algorithms), and AE31_W (AE31 data corrected by Weingartner algorithms) at 5 min time base. Here "/" denotes the AAE value calculated by the light absorption coefficients of two wavelengths (approach 1) and "-" denotes the AAE value obtained by curve fitting of seven wavelengths (approach 2).

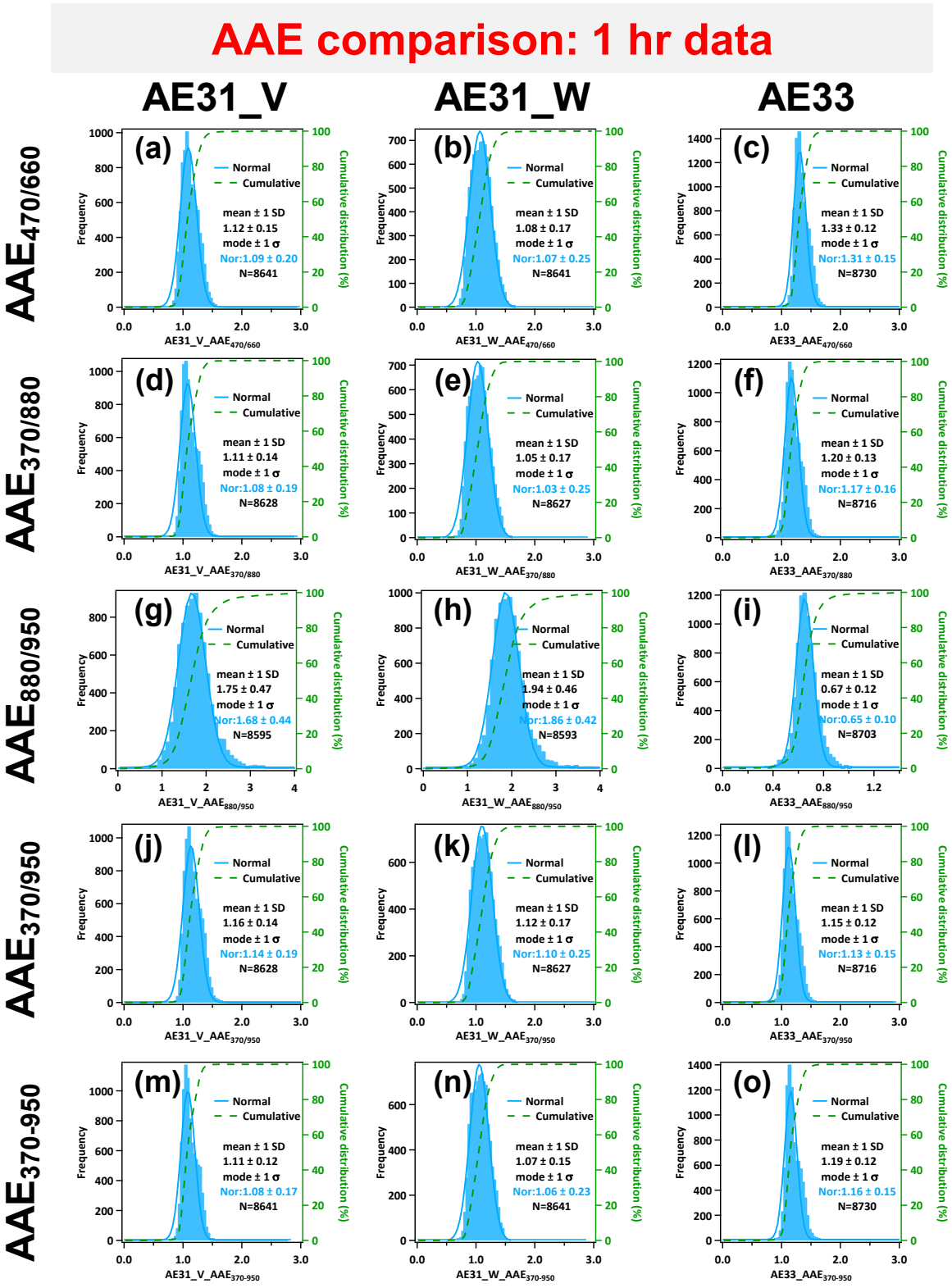

Figure S8. Frequency distributions of AAE values of AE33, AE31_V (AE31 corrected by the algorithms of Virkkula), and AE31_W (AE31 corrected by the algorithms of Weingartner) at 1 hr time base. Here "/" denotes the AAE value calculated by the light absorption coefficients of two wavelengths (approach 1) and "-" denotes the AAE value obtained by curve fitting of seven wavelengths (approach 2).

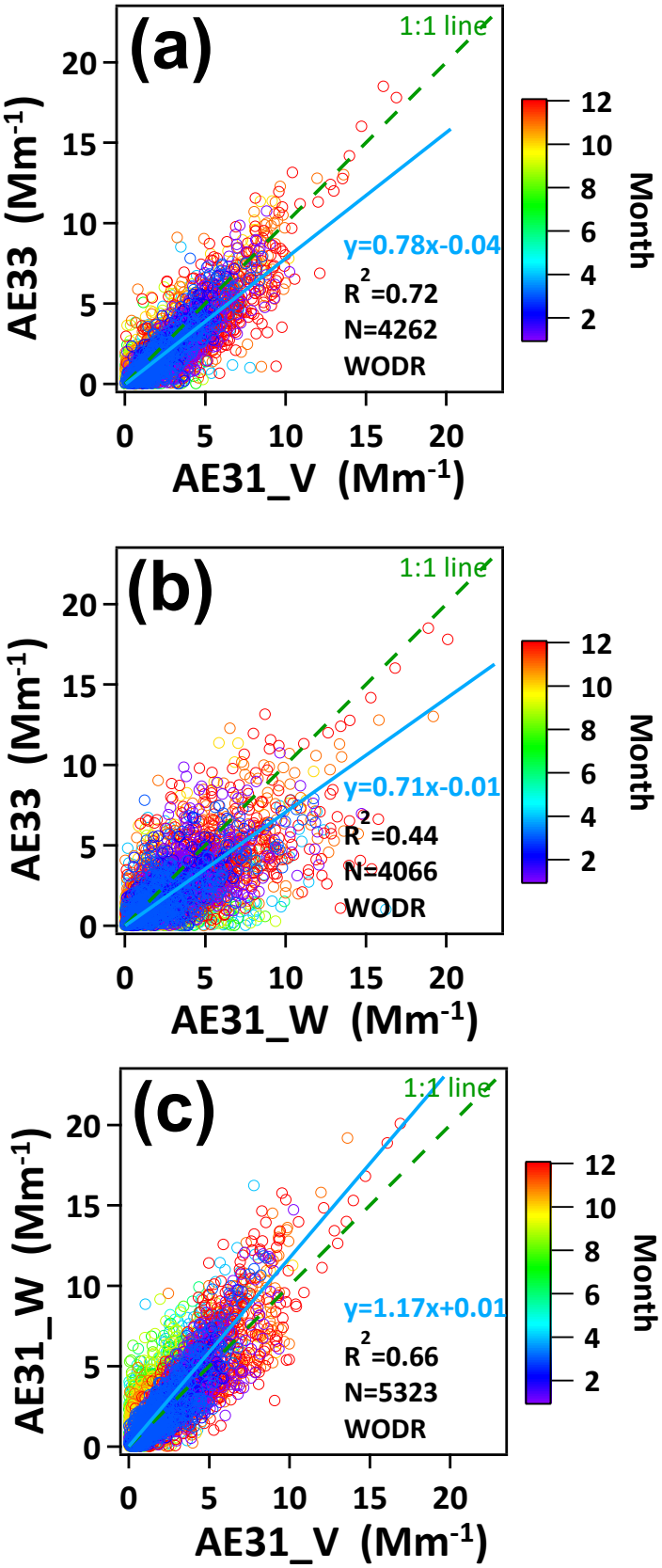

Figure S9. Scatter plot of b_{abs370_BrCsec} between AE31_V, AE31_W and AE33.

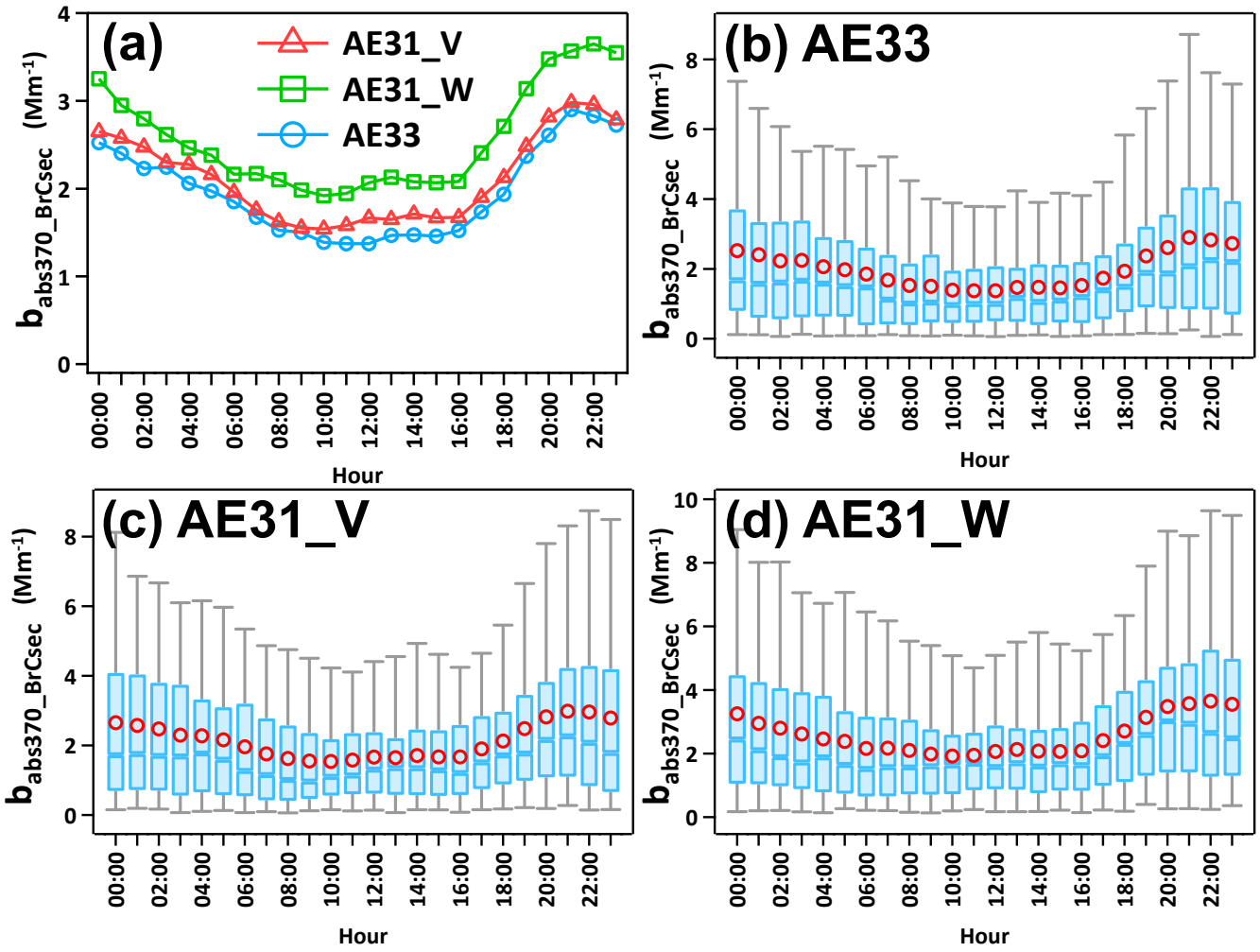

Figure S10. Diurnal variation of b_{abs370_BrCsec} with hourly time base. AE31_V and AE31_W represent the AE31 data corrected with algorithms of d and Weingartner, respectively.

References:

Ajtai, T., Kiss-Albert, G., Utry, N., Tóth, Á., Hoffer, A., Szabó, G., and Bozóki, Z.: Diurnal variation of aethalometer correction factors and optical absorption assessment of nucleation events using multi-wavelength photoacoustic spectroscopy, J. Environ. Sci., 83, 96-109, doi: https://doi.org/10.1016/j.jes.2019.01.022, 2019.

Arnott, W. P., Hamasha, K., Moosmüller, H., Sheridan, P. J., and Ogren, J. A.: Towards Aerosol Light-Absorption Measurements with a 7-Wavelength Aethalometer: Evaluation with a Photoacoustic Instrument and 3-Wavelength Nephelometer, Aerosol Science and Technology, 39, 17-29, doi: https://doi.org/10.1080/027868290901972, 2005.

Backman, J., Schmeisser, L., Virkkula, A., Ogren, J. A., Asmi, E., Starkweather, S., Sharma, S., Eleftheriadis, K., Uttal, T., Jefferson, A., Bergin, M., Makshtas, A., Tunved, P., and Fiebig, M.: On Aethalometer measurement uncertainties and an instrument correction factor for the Arctic, Atmos. Meas. Tech., 10, 5039-5062, doi: https://doi.org/10.5194/amt-10-5039-2017, 2017.

Bernardoni, V., Ferrero, L., Bolzacchini, E., Forello, A. C., Gregorič, A., Massabò, D., Močnik, G., Prati, P., Rigler, M., Santagostini, L., Soldan, F., Valentini, S., Valli, G., and Vecchi, R.: Determination of Aethalometer multiple-scattering enhancement parameters and impact on source apportionment during the winter 2017/18 EMEP/ACTRIS/COLOSSAL campaign in Milan, Atmos. Meas. Tech., 14, 2919-2940, doi: https://doi.org/10.5194/amt-14-2919-2021, 2021.

Collaud Coen, M., Weingartner, E., Apituley, A., Ceburnis, D., Fierz-Schmidhauser, R., Flentje, H., Henzing, J. S., Jennings, S. G., Moerman, M., Petzold, A., Schmid, O., and Baltensperger, U.: Minimizing light absorption measurement artifacts of the Aethalometer: evaluation of five correction algorithms, Atmos. Meas. Tech., 3, 457-474, doi: https://doi.org/10.5194/amt-3-457-2010, 2010.

Di Biagio, C., Formenti, P., Cazaunau, M., Pangui, E., Marchand, N., and Doussin, J. F.: Aethalometer multiple scattering correction Cref for mineral dust aerosols, Atmos. Meas. Tech., 10, 2923-2939, doi: https://doi.org/10.5194/amt-10-2923-2017, 2017.

Drinovec, L., Močnik, G., Zotter, P., Prévôt, A. S. H., Ruckstuhl, C., Coz, E., Rupakheti, M., Sciare, J., Müller, T., Wiedensohler, A., and Hansen, A. D. A.: The "dual-spot" Aethalometer: an improved measurement of aerosol black carbon with real-time loading compensation, Atmos. Meas. Tech., 8, 1965-1979, doi: https://doi.org/10.5194/amt-8-1965-2015, 2015.

Laing, J. R., Jaffe, D. A., and Sedlacek, I. I. I. A. J.: Comparison of Filter-based Absorption Measurements of Biomass Burning Aerosol and Background Aerosol at the Mt. Bachelor Observatory, Aerosol. Air. Qual. Res., 20, 663-678, doi: https://doi.org/10.4209/aaqr.2019.06.0298, 2020.

Lim, S., Lee, M., Kim, S.-W., and Laj, P.: Sulfate alters aerosol absorption properties in East Asian outflow, Scientific Reports, 8, 5172, doi: https://doi.org/10.1038/s41598-018-23021-1, 2018.

Qin, Y. M., Tan, H. B., Li, Y. J., Li, Z. J., Schurman, M. I., Liu, L., Wu, C., and Chan, C. K.: Chemical characteristics of brown carbon in atmospheric particles at a suburban site near Guangzhou, China, Atmos. Chem. Phys., 18, 16409-16418, doi: https://doi.org/10.5194/acp-18-16409-2018, 2018.

Saturno, J., Pöhlker, C., Massabò, D., Brito, J., Carbone, S., Cheng, Y., Chi, X., Ditas, F., Hrabě de Angelis, I., Morán-Zuloaga, D., Pöhlker, M. L., Rizzo, L. V., Walter, D., Wang, Q., Artaxo, P., Prati, P., and Andreae, M. O.: Comparison of different Aethalometer correction schemes and a reference multi-wavelength absorption technique for ambient aerosol data, Atmos. Meas. Tech., 10, 2837-2850, doi: https://doi.org/10.5194/amt-10-2837-2017, 2017.

Schmid, O., Artaxo, P., Arnott, W. P., Chand, D., Gatti, L. V., Frank, G. P., Hoffer, A., Schnaiter, M., and Andreae, M. O.: Spectral light absorption by ambient aerosols influenced by biomass burning in the Amazon

Basin. I: Comparison and field calibration of absorption measurement techniques, Atmos. Chem. Phys., 6, 3443-3462, doi: https://doi.org/10.5194/acp-6-3443-2006, 2006.

Segura, S., Estellés, V., Titos, G., Lyamani, H., Utrillas, M. P., Zotter, P., Prévôt, A. S. H., Močnik, G., Alados-Arboledas, L., and Martínez-Lozano, J. A.: Determination and analysis of in situ spectral aerosol optical properties by a multi-instrumental approach, Atmos. Meas. Tech., 7, 2373-2387, doi: https://doi.org/10.5194/amt-7-2373-2014, 2014.

Valentini, S., Barnaba, F., Bernardoni, V., Calzolai, G., Costabile, F., Di Liberto, L., Forello, A. C., Gobbi, G. P., Gualtieri, M., Lucarelli, F., Nava, S., Petralia, E., Valli, G., Wiedensohler, A., and Vecchi, R.: Classifying aerosol particles through the combination of optical and physical-chemical properties: Results from a wintertime campaign in Rome (Italy), Atmospheric Research, 235, 104799, doi: https://doi.org/https://doi.org/10.1016/j.atmosres.2019.104799, 2020.

Weingartner, E., Saathoff, H., Schnaiter, M., Streit, N., Bitnar, B., and Baltensperger, U.: Absorption of light by soot particles: determination of the absorption coefficient by means of aethalometers, J. Aerosol. Sci., 34, 1445-1463, doi: https://doi.org/10.1016/S0021-8502(03)00359-8, 2003.

Wu, D., Wu, C., Liao, B., Chen, H., Wu, M., Li, F., Tan, H., Deng, T., Li, H., Jiang, D., and Yu, J. Z.: Black carbon over the South China Sea and in various continental locations in South China, Atmos. Chem. Phys., 13, 12257-12270, doi: https://doi.org/10.5194/acp-13-12257-2013, 2013.

Zhang, Y., Zhi, G., Jin, W., Liu, S., Wang, L., Li, Z., Shi, R., Zhang, P., Shu, Y., and Hu, J.: Developing a dynamic correction mechanism for aethalometer results of actual urban aerosols, Atmos. Res., 255, 105529, doi: https://doi.org/10.1016/j.atmosres.2021.105529, 2021.

Zhao, G., Yu, Y., Tian, P., Li, J., Guo, S., and Zhao, C.: Evaluation and Correction of the Ambient Particle Spectral Light Absorption Measured Using a Filter-based Aethalometer, Aerosol and Air Quality Research, 20, 1833-1841, doi: https://doi.org/10.4209/aaqr.2019.10.0500, 2020.